

Supplementary Information

Do very small POSS nanoparticles perturb s-PMMA conformation?

Nicolas Jouault,^{1*} Sanat K. Kumar,² Robert J. Smalley,³ Changzai Chi,³ Robert Moneta,³ Barbara Wood,³ Holly Salerno,³ Yuri B. Melnichenko,⁴ Lilin He,⁴ William E. Guise,^{3,5} Boualem Hammouda⁶,
and Michael K. Crawford^{3,7*}

¹Sorbonne Université, CNRS, Laboratoire Physicochimie des Electrolytes et des Nanosystèmes Interfaciaux, PHENIX, F-75005 Paris, France

²Department of Chemical Engineering, Columbia University, New York, N.Y 10027, USA

³DuPont Central Research and Development, E400/5424, Wilmington, DE 19880-0400, USA

⁴Neutron Scattering Division, Oak Ridge National Laboratory, Oak Ridge, TN 37831-6393, USA

⁵Advanced Photon Source, Argonne National Laboratory, 9700 S. Cass Ave, Lemont, IL 60439, USA

⁶NIST Center for Neutron Research, Gaithersburg, MD 20879-8562, USA

⁷Department of Physics and Astronomy, University of Delaware, Newark, DE 19716, USA

Corresponding author:

(MKC): mkcrawford987@gmail.com

(NJ): nicolas.jouault@sorbonne-universite.fr

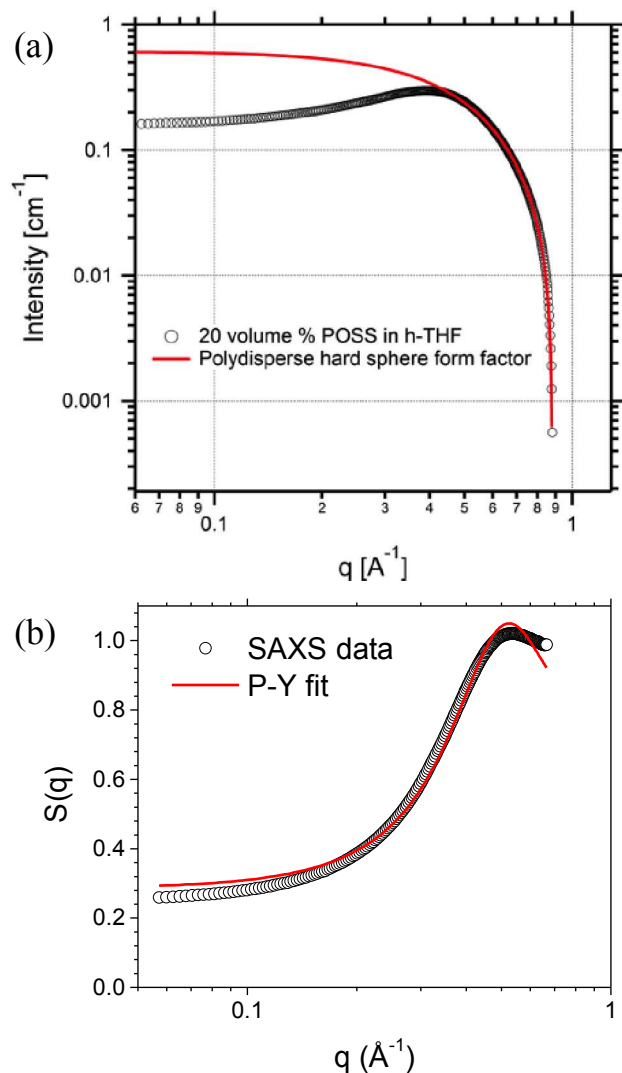


Figure S1. (a) SAXS scattering intensity as a function of scattering vector q (black open circles) for a 20 % v/v POSS MS0815 solution in THF. The data at high q are fit (red curve) to a lognormal distribution of NP radii with nearly zero polydispersity. The particle diameter from the fit is 0.83 nm. The large deviation of the fit from the data with decreasing q is due to structure factor effects resulting from the high POSS concentration. (b) Structure factor $S(q)$ derived by dividing data from (a) by the form factor for a hard sphere of diameter 0.83 nm, determined from the fit in (a). The effective diameter of the POSS hard sphere derived from the Percus-Yevick structure factor is 1.13 nm, showing the contribution of the organic ligands to the hard sphere repulsion, and thus the effective POSS diameter, when compared to the

POSS diameter of 0.83 nm derived from the fit to the high q region of the single particle form-factor shown in (a). When a hard sphere form factor is fit to the SAXS data, the resulting effective particle size is sensitive to the x-ray scattering length density contrast between the POSS Si_8O_{12} cage, the POSS ligands and the surrounding THF solvent, As a result, x-rays primarily see the POSS Si_8O_{12} cage and not the organic ligands, the latter which have x-ray scattering length densities that are similar to the THF solvent. The structure factor, however, is sensitive to the “true” POSS hard sphere diameter since it reflects interference between X-rays scattered by different POSS molecules. The distribution of distances between NPs determines the interparticle scattering, so the structure factor can be used to estimate the hard sphere diameter of NPs.

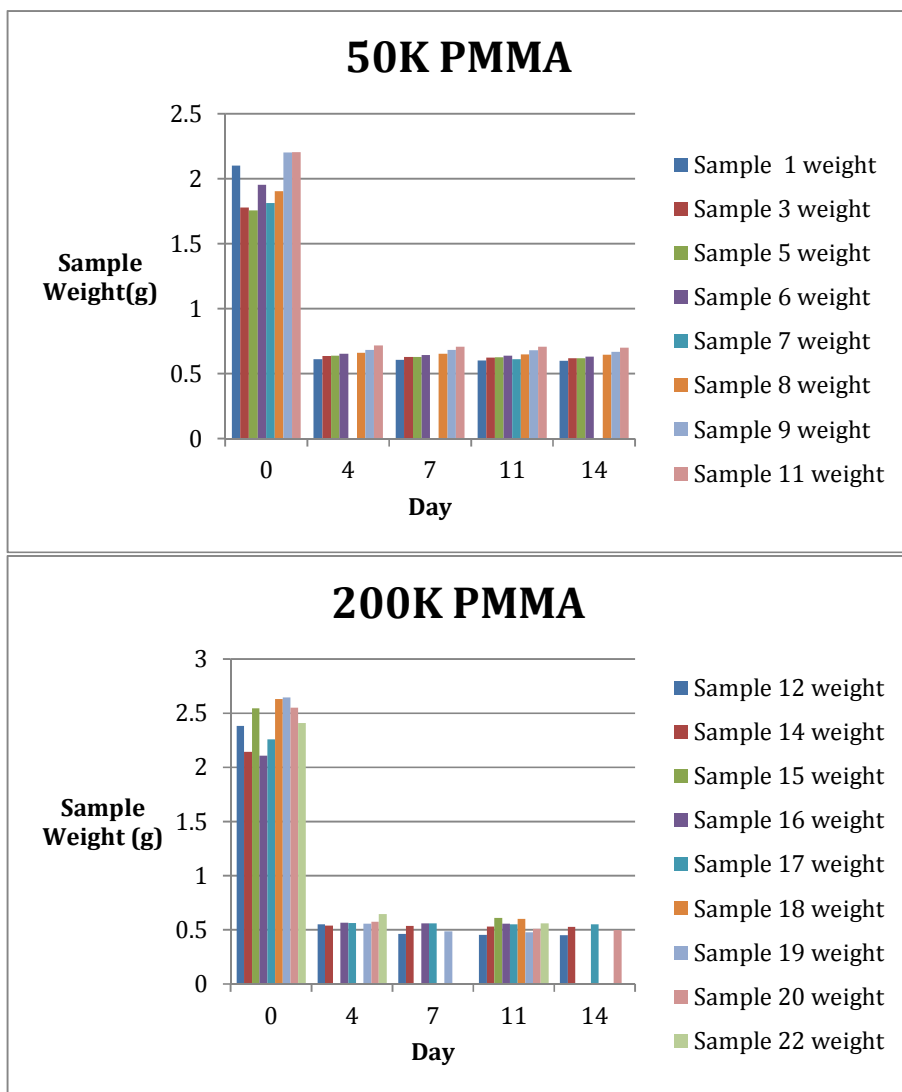


Figure S2. Weight evolution at room temperature for a period of 0 -14 days for POSS/PMMA PNCs listed in Table S1 (Top: 50 kDa, Bottom: 200 kDa). The data show no significant variation of retained solvent content with POSS concentration. There is also no obvious effect of polymer molecular weight (the percent solids for the 200 kDa sample solutions was initially lower than for the 50 kDa samples, so the starting solution volume was increased to obtain roughly the same mass of PNC after solvent evaporation).

Table S1. List of samples whose weights were monitored by TGA and the results plotted in Figure S2. The d-PMMA and h-PMMA volume fractions only refer to the polymer volume fractions; they should be multiplied by (1-POSS volume fraction) to convert to polymer component volume fraction of total nanocomposites (ignoring the possible presence of some residual solvent).

Sample Number	Approximate M_w PMMA (kDa)	Volume Fraction POSS MS0815	Volume Fraction d-PMMA	Volume Fraction h-PMMA
1	50	0	0.097	0.903
3	50	0.05	0.097	0.903
5	50	0.05	1	0
6	50	0.1	0.097	0.903
7	50	0.1	0.25	0.75
8	50	0.1	1	0
9	50	0.2	0.097	0.903
11	50	0.2	1	0
12	200	0	0.097	0.903
14	200	0.05	0.097	0.903
15	200	0.05	0.25	0.75
16	200	0.05	1	0
17	200	0.1	0.097	0.903
18	200	0.1	0.25	0.75
19	200	0.1	1	0
20	200	0.2	0.097	0.903
22	200	0.2	1	0

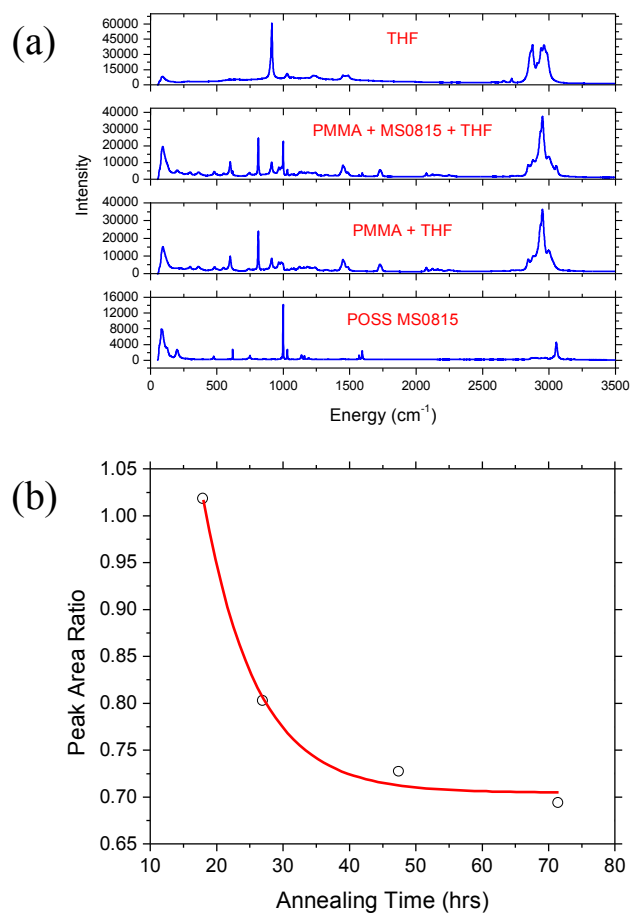


Figure S3. (a) Raman spectra of THF; a 50 kDa PMMA/10 % v/v POSS MS0815 nanocomposite with residual THF (sample 6 in Table S1); the same 50 kDa PMMA polymer without POSS but with residual THF (sample 1 in Table S1); and POSS MS0815. The strongest Raman transitions of the POSS near 1,000 cm⁻¹ and THF at 912 cm⁻¹ can be clearly seen in the nanocomposites spectrum, while the THF Raman transition also appears in the pure PMMA spectrum, which was cast from a PMMA/THF solution. (b) Loss of THF from a 120 kDa PMMA film at room temperature, determined by measuring spectra that included a THF Raman peak at 812 cm⁻¹ and a PMMA peak at 912 cm⁻¹. Integrated intensity ratios, or the areas of these two peaks, scale directly with the volume fraction of THF in the films and

can thus be used to monitor THF loss quantitatively, but still require calibration against some other measure of solvent loss such as TGA.

PMMA M_w	POSS volume fraction (%)	Normalization factor
50 kDa	5	1.13
	10	1.10
	20	1.35
193 kDa	5	1
	10	1
	20	1
500 kDa	5	1
	10	1.15
	20	1.15

Table S2: SANS normalization factors for the different systems.

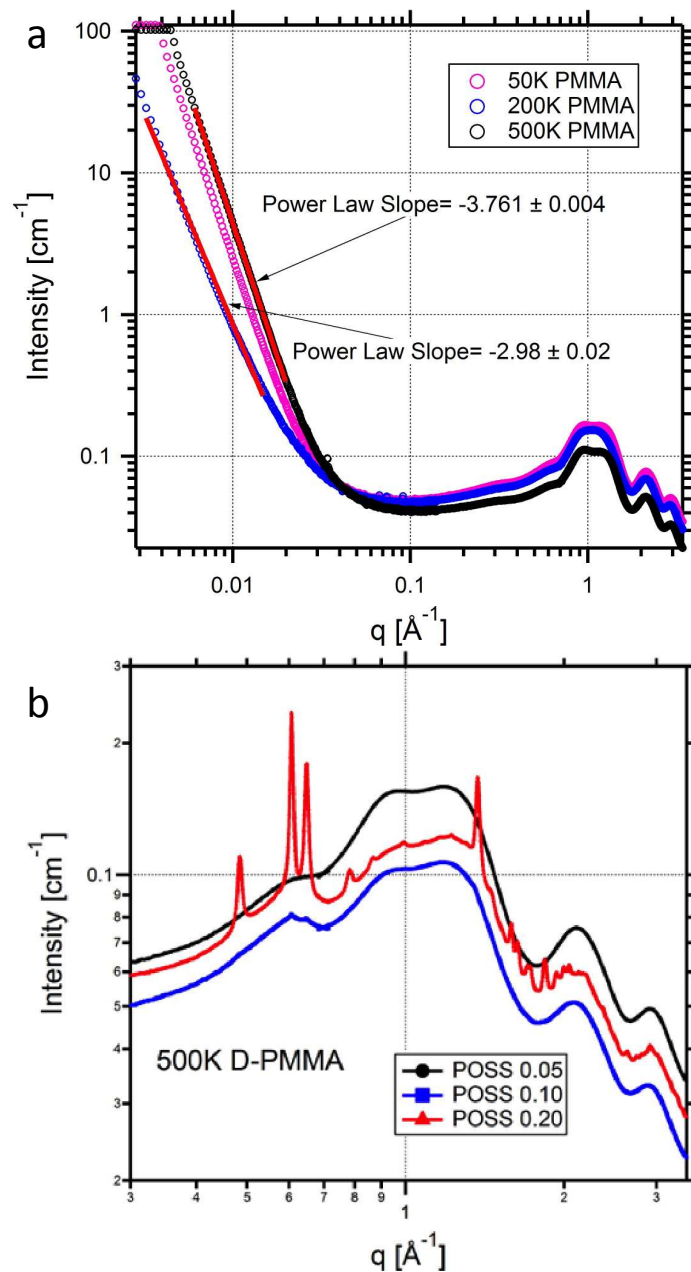


Figure S4. (a) SAXS data for 90.3 % v/v h-PMMA / 9.7 % v/v d-PMMA samples with three molecular weights (50 kDa, 200 kDa and 500 kDa). All three samples show large upturns at low q , which clearly shows that the upturns observed in the PNCs are not due to POSS aggregation. The power law slopes vary from q^{-3} to $q^{-3.76}$, consistent with scattering from

crazes with varying boundary sharpness profiles¹. (b) WAXS data for 500 kDa d-PMMA PNCs (5 %, 10 % and 20 % v/v POSS).

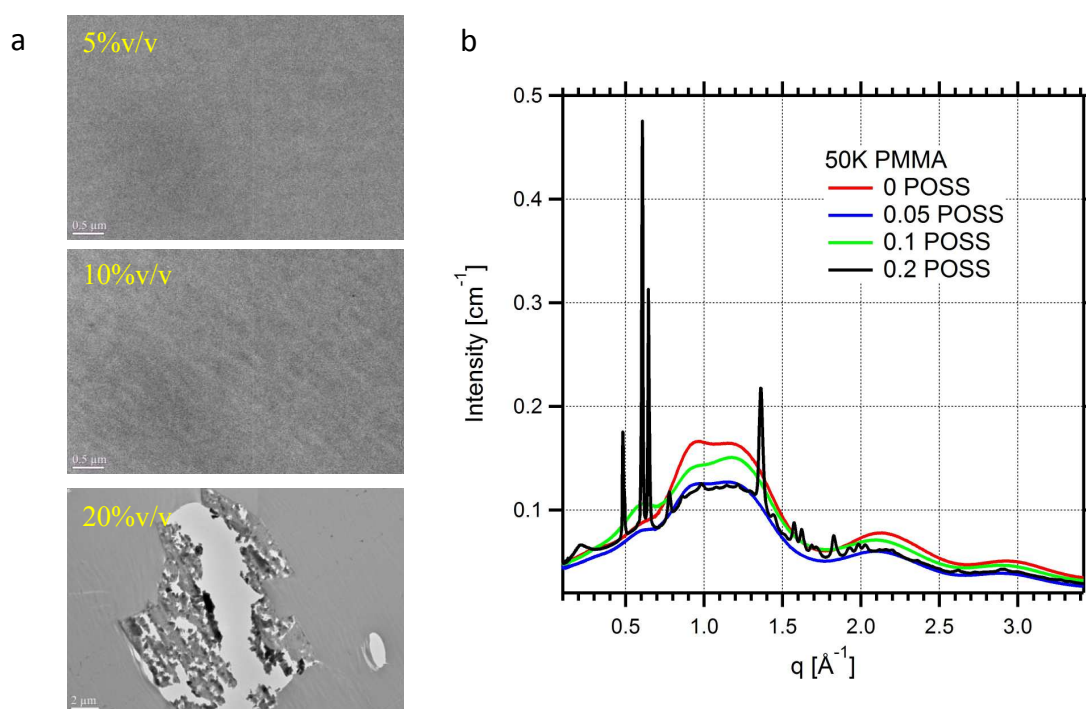


Figure S5. (a) TEM images of 50 kDa 90.3 % v/v h-PMMA / 9.7 % v/v d-PMMA PNCs filled with 5 % (top), 10 % (middle) and 20 % v/v (bottom) POSS. (b) WAXS spectra of unfilled (0 %) and filled (5 %, 10 % and 20 % v/v) POSS/PMMA PNCs.

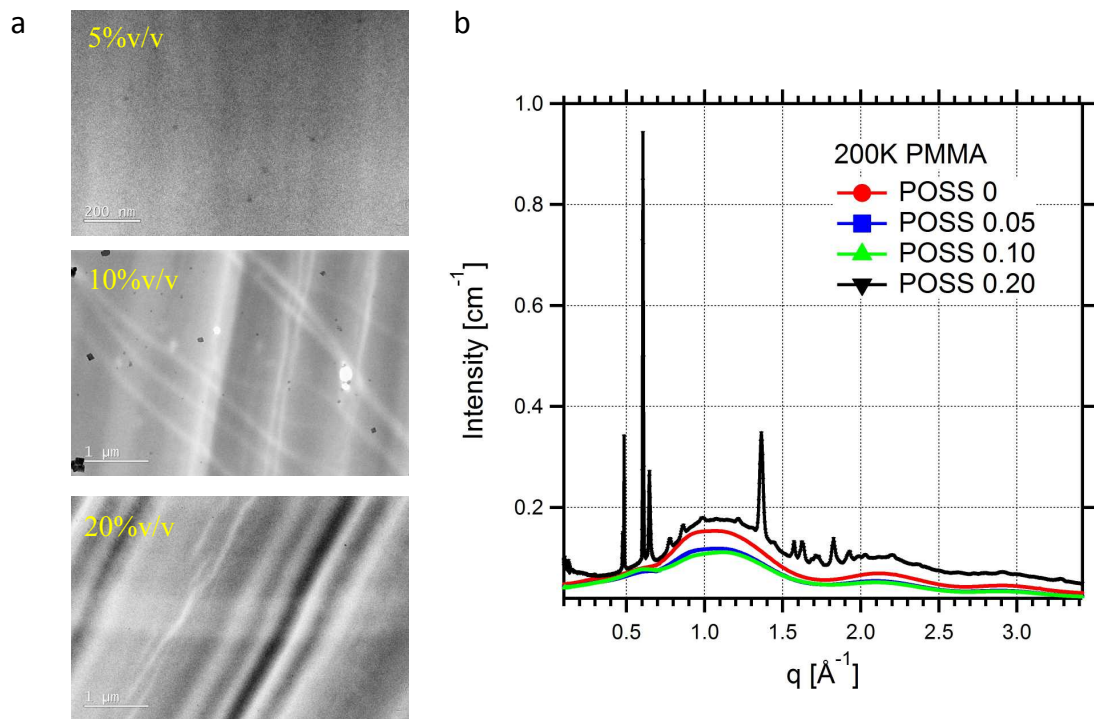
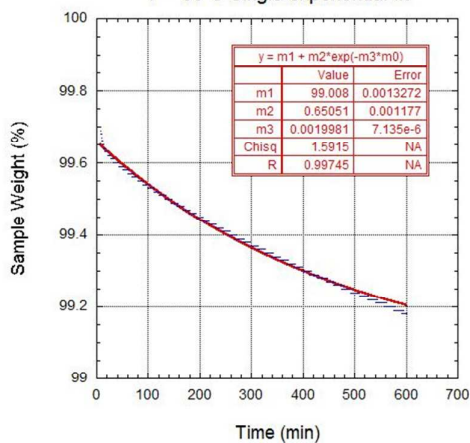
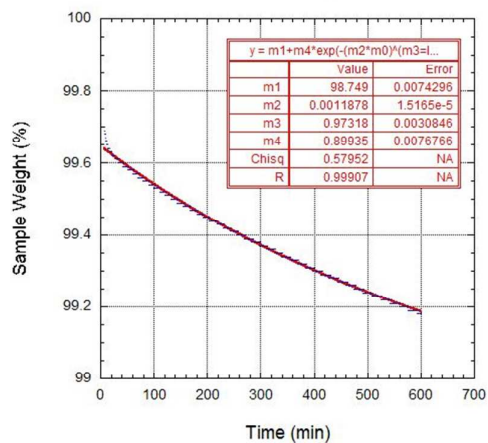


Figure S6. (a) TEM images of 193 kDa 90.3 % v/v h-PMMA / 9.7 % v/v d-PMMA PNCs filled with 5 % (top), 10 % (middle) and 20 % v/v (bottom) POSS. (b) WAXS spectra of unfilled (0 volume fraction) and filled (5 %, 10 % and 20 % v/v) POSS/PMMA PNCs.

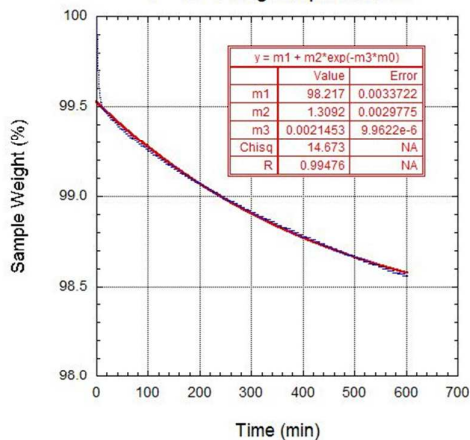
T = 50 C Single exponential fit



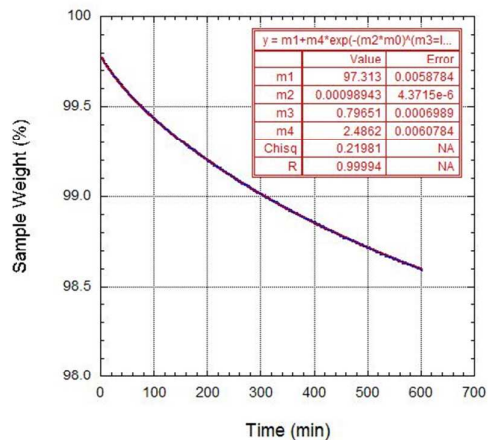
T = 50 C Stretched exponential fit



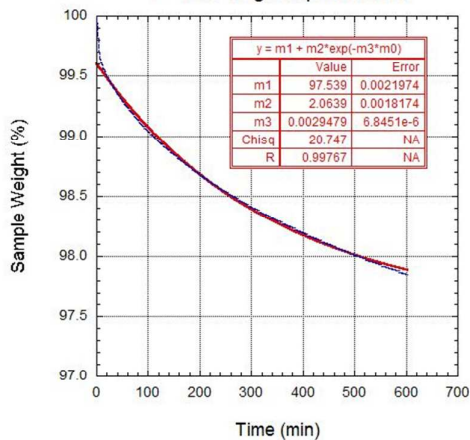
T = 60 C Single exponential fit



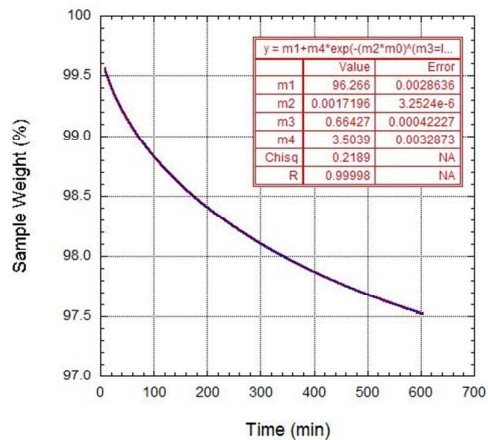
T = 60 C Stretched exponential fit



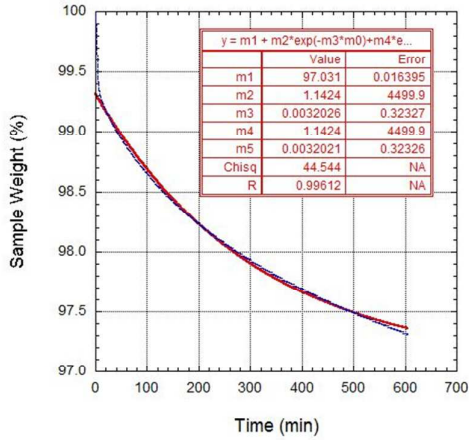
T = 70C Single exponential fit



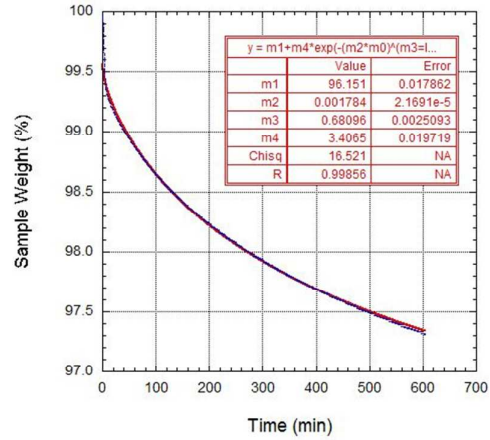
T = 70 C Stretched exponential fit



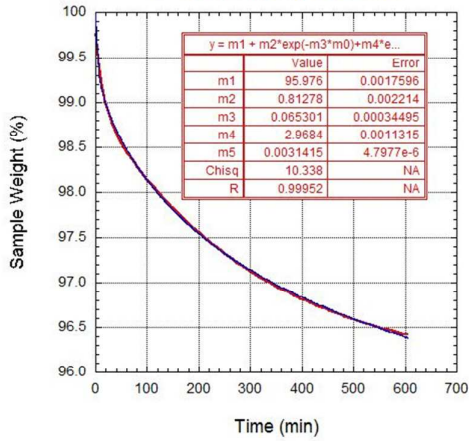
T = 80 C Two exponential fit



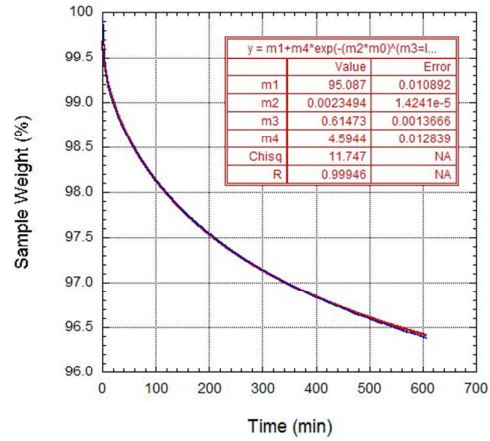
T = 80 C Stretched exponential fit



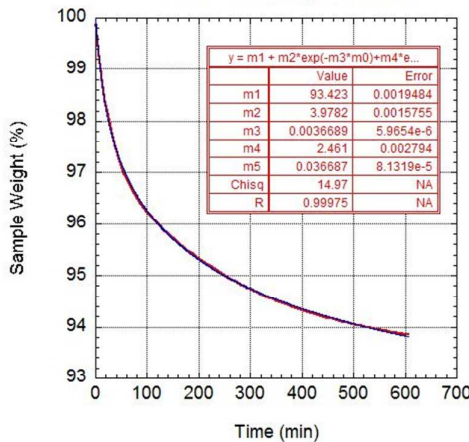
T = 90 C Two exponential fit



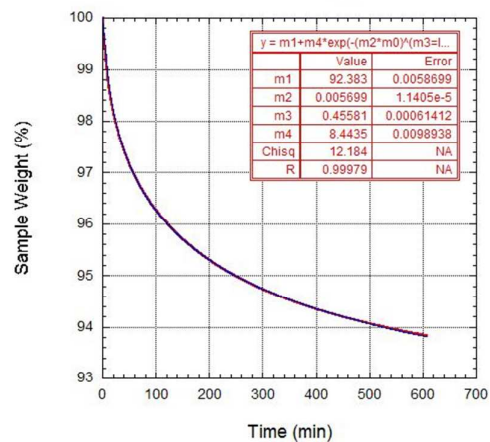
T = 90 C Stretched exponential fit



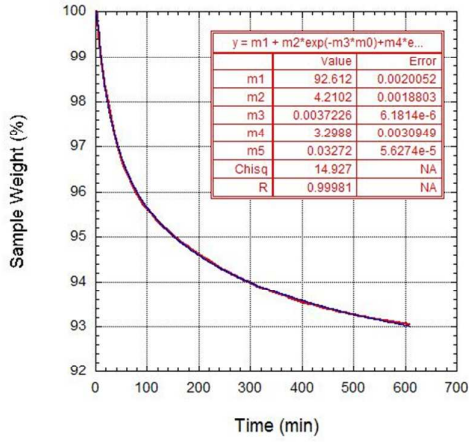
T = 110 C Two exponential fit



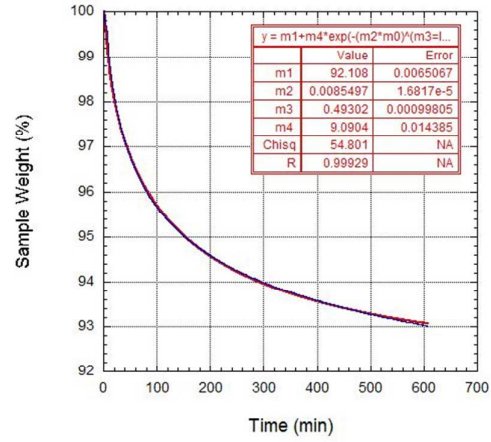
T = 110 C Stretched exponential fit



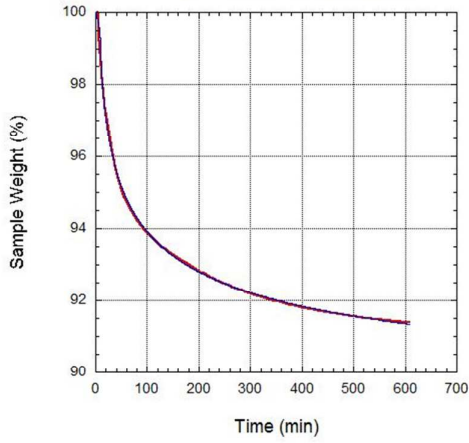
T = 120 C Two exponential fit



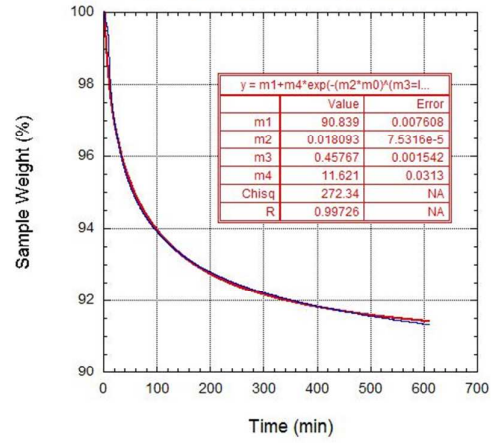
T = 120 C Stretched exponential fit



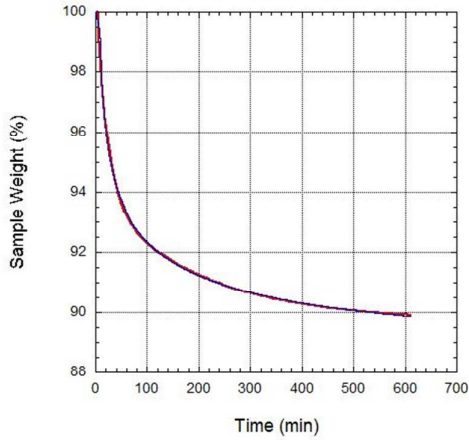
T = 130 C Two exponential fit



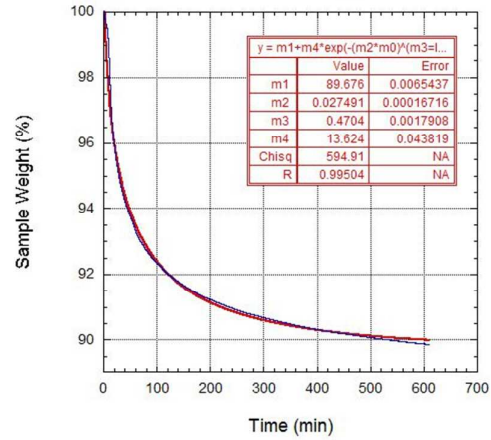
T = 130 C Stretched exponential fit



T = 140 C Two exponential fit



T = 140 C Stretched exponential fit



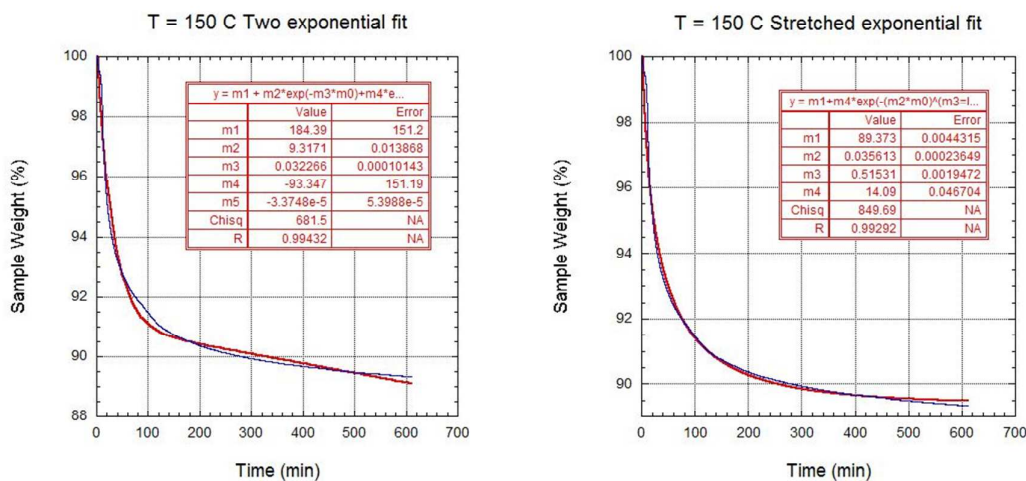


Figure S7. A series of isothermal TGA traces measured for PMMA samples cast from PMMA/THF solutions, followed by air drying at room temperature (20 °C) for 48 hours, nearly enough time for the THF content to reach equilibrium. The PMMA had an average $M_w = 120$ kDa by GPC and a $T_g = 105$ °C by DSC (midpoint temperature of about 120 °C). The TGA data were collected using a TA Instruments Q5000 TGA. The heating rate was 10 °C/min and the samples were heated under a N_2 purge. Each sample was run three times, using 10 hour hold times at 50, 60, 70, 80, 90, 110, 120, 130, 140 and 150 °C.

Each trace shows sample weight versus time at a specific fixed temperature. Superimposed on each experimental curve is a fit to either a single exponential decay at (50, 60, 70 °C), $y = m_1 + m_2 e^{-(m_3 t)}$; a double exponential decay at (80, 90, 110, 140 °C), $y = m_1 + m_2 e^{-(m_3 t)} + m_4 e^{-(m_5 t)}$; or a single stretched exponential decay at all temperatures, $y = m_1 + m_4 e^{-(m_2 t)^{m_3}}$. The stretching exponent m_3 varies from approximately 1.0 to 0.5 as a function of temperature from 50 °C to 150 °C. This is consistent with a picture where the solvent (THF) diffusion in the glassy phase is essentially controlled by the tortuosity of the diffusion path in a stationary polymer matrix, yielding a single exponential decay, whereas in the rubbery phase above T_g polymer dynamics become an important perturbation on the

diffusion process leading to a stretched exponential behaviour representing a distribution of relaxation times.

Diffusion coefficient of THF in 120K PMMA

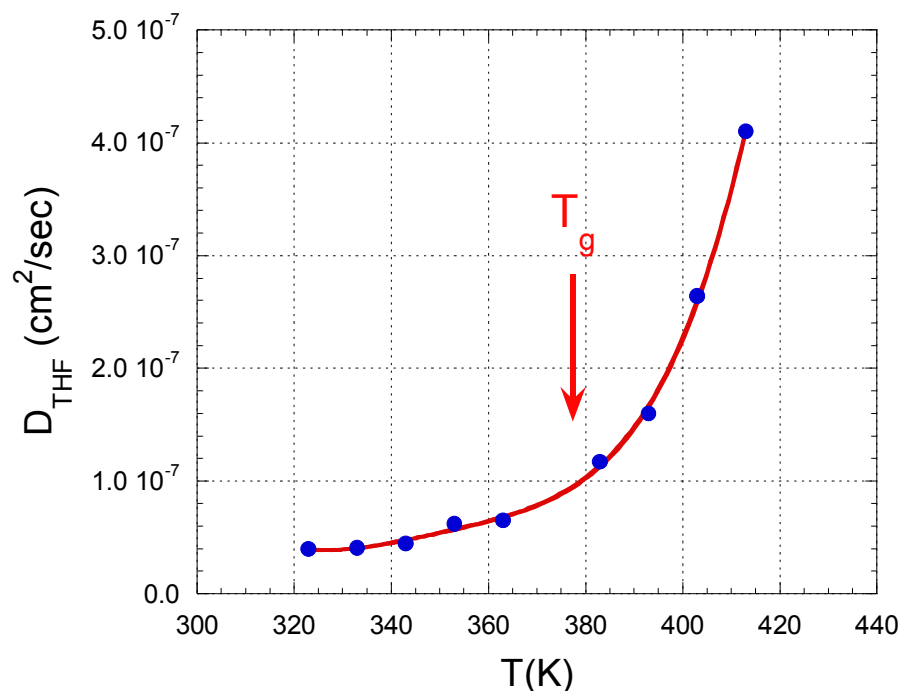


Figure. S8. Diffusion coefficient of THF in 120 kDa PMMA determined from the single and double exponential fits to the thermogravimetry data shown in Fig. S7. These numbers should be compared to the self-diffusion coefficient of THF, which we assume is equal to those of other similarly-sized molecules such as acetone or t-butyl acetate. We assumed that the samples were thin enough (0.1 mm) that the diffusion is essentially one-dimensional. In that case, the time for the THF concentration in the film to change half as much as required to reach the equilibrium concentration of THF in PMMA at that temperature, is equal to $0.04919 \times t^2/D$, where D is the THF diffusion coefficient at that temperature and t is the film thickness². Applying that expression to the data in Figure S7 led to the D_{THF} values shown in Figure S8.

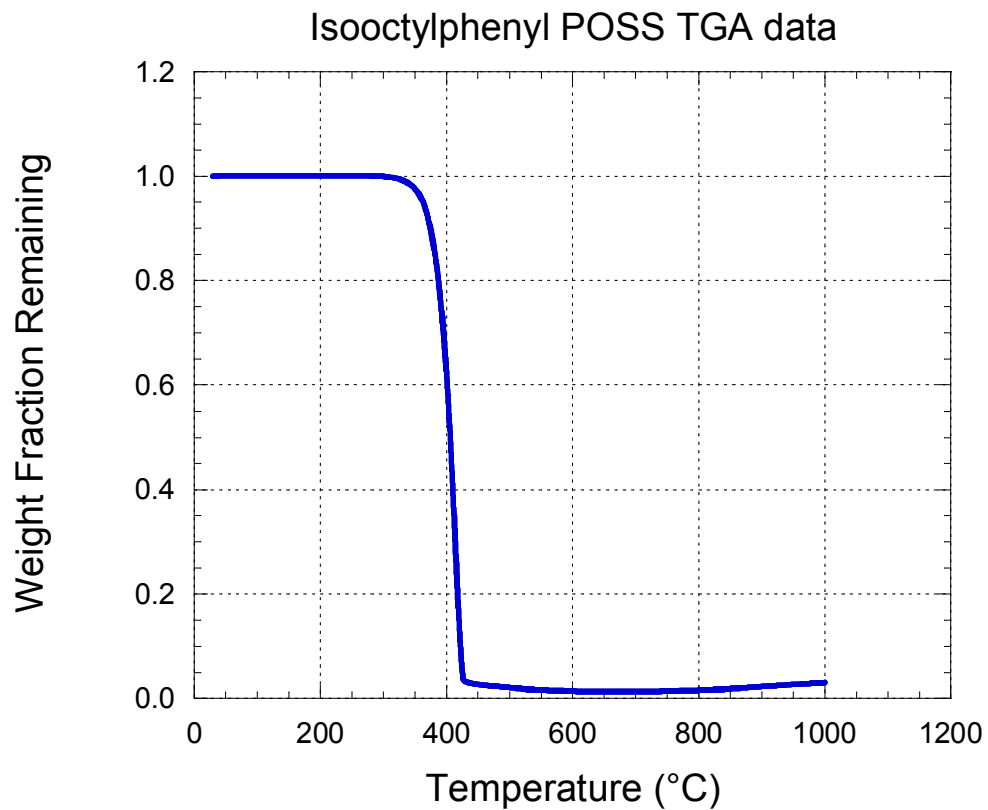


Figure. S9. TGA data for a sample of isooctylphenyl POSS (MS0815) showing thermal stability to a temperature of approximately 300 °C, well above any PNC annealing temperatures used in this study. Above that temperature the POSS NPs either decompose or sublime, leaving very little residue.

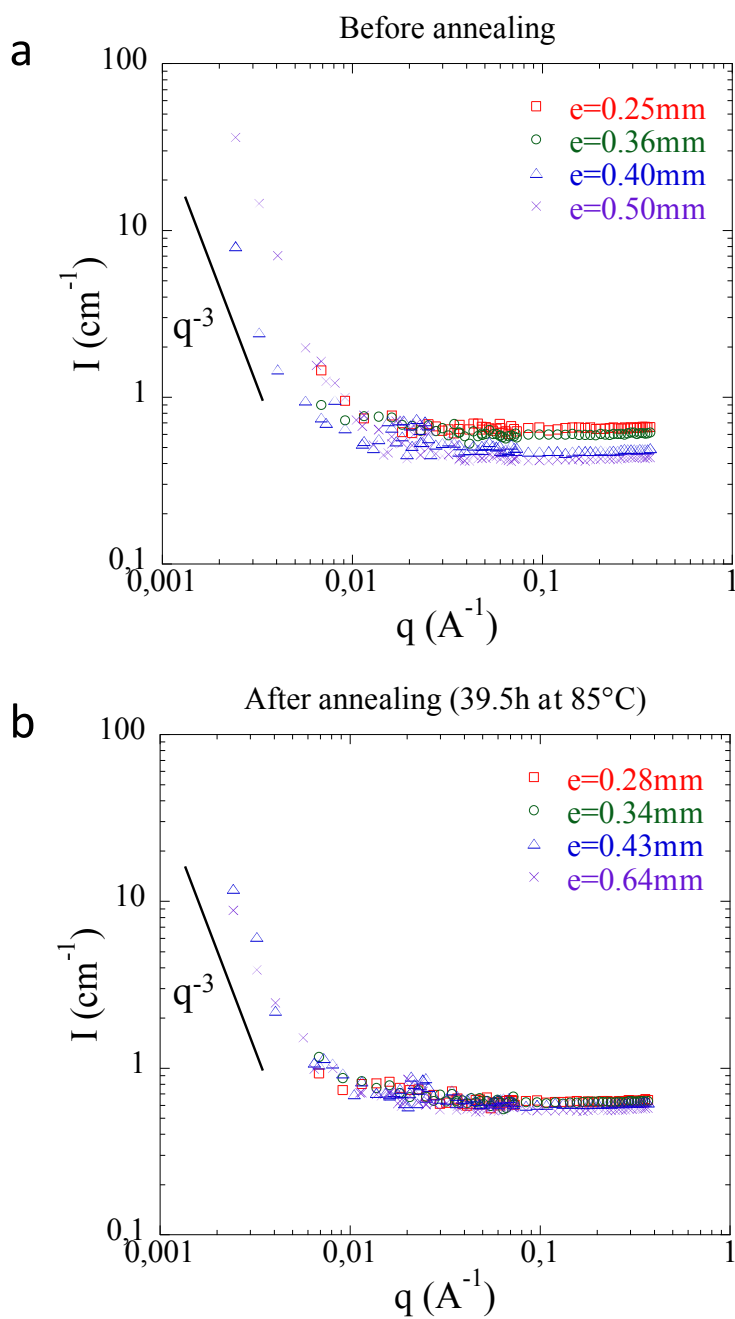


Figure S10. Scattering intensity $I(q)$ as a function of scattering vector q for pure h-PMMA with average $M_w = 120$ kDa at different thicknesses before annealing (a) and after annealing (b). The samples were prepared by solvent casting method using THF.

References

1. Salomons, G.; Singh, M.; Bardouille, T.; Foran, W.; Capel, M. Small-angle X-ray scattering analysis of craze-fibril structures. *Journal of applied crystallography* **1999**, 32 (1), 71-81.
2. Balik, C. On the extraction of diffusion coefficients from gravimetric data for sorption of small molecules by polymer thin films. *Macromolecules* **1996**, 29 (8), 3025-3029.